

Hot roller embossing for microfluidics: process and challenges

S. H. Ng · Z. F. Wang

Received: 1 June 2008 / Accepted: 8 October 2008 / Published online: 28 October 2008
© Springer-Verlag 2008

Abstract We report an initial study on hot roller embossing as a potential process for the mass production of polymer based microfluidic chips. Measurements conducted on 100 μm features showed that the lateral dimensions could be replicated to within 2% tolerance, while over 85% of mould depth was embossed. Feature sizes down to 50 μm and feature depths up to 30 μm had been achieved. Results revealed that the embossing depth increased with an increase in the nip force or a decrease in the rolling speed. There was an optimum temperature for achieving a high embossing depth; this was due to the reflow effect seen at higher temperatures. One observation included an asymmetric pile up of polymer material outside the embossed regions as a result of the orientation of the microchannel with respect to the rolling direction. This directional effect could be due to the dynamics of the roller setup configuration.

1 Introduction

Low-cost, disposable microfluidic chips have application in point of care (POC) and mass screening operations where large quantities are required. The “use and dispose” strategy is similar in other medical devices such as the plastic syringes and hypodermic needles so that contamination due to reuse and inadequate cleaning or sterilization is eliminated. Polymer has always been the material of choice when applications require mass quantities at low

cost, due to its low material cost and the associated mass production processes such as injection moulding. Commonly used polymers for microfluidics—such as polymethyl methacrylate (PMMA) and polycarbonate (PC)—face some drawbacks in terms of maximum operating temperature, gas permeability, structural strength, optical properties and chemical resistance when compared to silicon and glass. Recent advancement in polymer chemistry has produced some high-performance polymers such as polyetheretherketone (PEEK) and cyclic olefin copolymer (COC), that can withstand higher temperatures and harsher chemical environment.

Polymer replication techniques such as hot embossing, injection moulding and soft lithography have traditionally been popular for the manufacturing of microfluidic chips. All these are mould based methods for creating open microchannels and cavities on polymer surfaces. Subsequent bonding with another piece of polymer will form the embedded microchannels and cavities. Emerging technologies include roll replication techniques such as ultraviolet (UV) roller embossing and hot roller embossing. Roller replication techniques have their attractiveness in mass production and compatibility with other reel-to-reel processes such as gravure or flexo printing for the creation of conductive elements, and lamination for sealing and encapsulation. UV roller embossing uses UV light to cure a thin film of photopolymer while hot roller embossing relies on heat and pressure to form the polymer. While UV roller embossing has the advantage of lower pressure and no heating requirement, there are limitations in terms of film thickness, chemical resistance and optical properties, due to the nature of the process and the properties of the UV curable resin. Hot roller embossing has its issues as well in terms of higher operating temperature, higher contact pressure, speed and other issues. In this study, some initial

S. H. Ng (✉) · Z. F. Wang
Singapore Institute of Manufacturing Technology,
71 Nanyang Drive, Singapore 638075, Singapore
e-mail: shng@simtech.a-star.edu.sg

studies and considerations of the hot roller embossing will be reported.

There is some related research on hot roller embossing in the literature. Tan et al. (1998) performed roller nano-imprint lithography on thin coatings of photoresist that are hundreds of nanometers in thickness. They reported the advantage of using less force over a large substrate. However, their sample size was limited to a couple of centimetres and their setup could not perform continuous operation. Schiff et al. (2006) reported on the surface structuring of textile fibres using roll embossing. Sub-micron periodic structures were transferred from a thin metal shim (the mould) onto the surface of polyester fibres that were 180 μm in diameter. While roller embossing can achieve very high production rates (in excess of 1,000 mm/s for plastic foil of up to 2 m width), the replication of microstructures with deep relief ($>1 \mu\text{m}$) is not yet an established mass-production process (Herzig 1997). The hot embossing of polymer foil, or even metallized polymer foil, is well established and widely used for mass-producing foils for markets ranging from wrapping and packaging to diffractive optical elements, but with feature relief depth of only up to 1 μm (Gale et al. 2005). The fidelity of replicated nano or microstructures is very dependent upon the aspect ratio (feature height to width). A general rule of thumb is that an aspect ratio of 1:1 can be replicated easily, 5:1 with care and 10:1 only with great difficulty. The issue with aspect ratio arises at both the moulding and demoulding steps of the process.

2 Hot roller embossing

While previous study focused on the nanometer or sub-micron scale, we work on the micrometre scale typical of microfluidics structures. In our approach (see Fig. 1), a thermoplastic sheet is passed between two rollers. The top roller is made of steel with a nickel film mould mounted while the bottom roller is a rubber support roller. Heat is supplied to the embossing interface through the mould and a clamping pressure is applied between the two rollers. As the substrate passes between the rollers, the mould features are embossed into it. Preheating of the substrate can also be conducted before it is fed into the rollers. The process is different from hot embossing where the polymer substrate is given ample time to heat up and cooling is carried out with the force still applied. Table 1 lists some differences between the conventional hot embossing (Ng et al. 2007) that uses a flat, rigid mould and hot roller embossing. Typically, conventional hot embossing can give a better replication of the mould because the polymer can be demoulded at a temperature below its glass transition temperature, minimizing any polymer flow after the mould

is removed. The trade off is a longer process time as compared to hot roller embossing.

3 Experimental

A 50 μm thick nickel mould (see Fig. 1b) with raised microstructures fabricated by electroplating process was wrapped around the top stainless steel roller that could be internally heated up to 177°C. The fabrication of the film mould poses a challenge especially when the area is large. Figure 2 shows the fabrication process of the mould. The base mould is first electroplated followed by photoresist patterning. Further electrolytic plating will result in the filling up of the cavities around the photoresist. When the required height of the mould feature is reached, the electroplating process is stopped and the photoresist removed by chemicals. The piece of nickel shim is then trimmed to final size by laser cutting and then mounted onto the roller embossing machine.

Figure 3 shows scanning electron micrographs of the features on the mould. The features consisted of line arrays with different line width and pattern density, as well as microchannel designs (not shown). The smallest feature size was 50 μm . As seen in Fig. 4a, the surface roughness of the mould base was $\sim 0.1 \mu\text{m}$. For better optical clarity, the

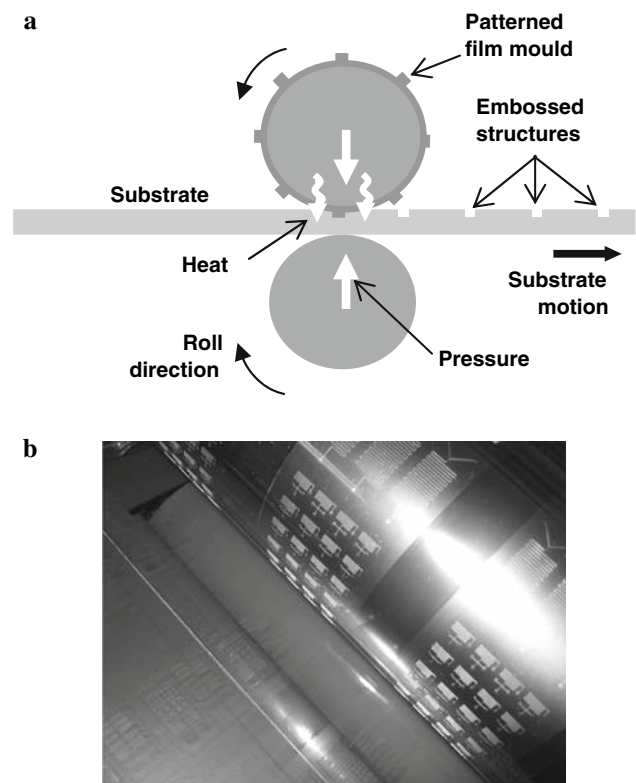
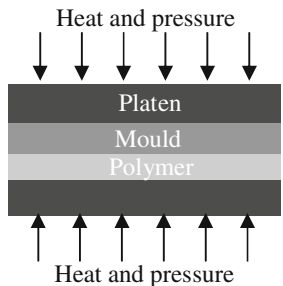
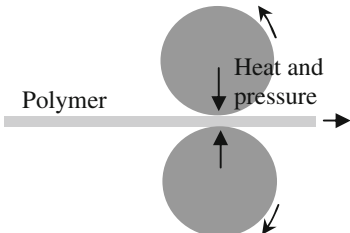


Fig. 1 Hot roller embossing process

Table 1 A few differences between conventional hot embossing that uses a flat, rigid mould and hot roller embossing

	Conventional hot embossing	Hot roller embossing
		
Mould	Flat and rigid mould (typically electroformed nickel a few millimeters in thickness)	Typically a metal shim (tens to hundreds of microns thick) mounted on a rigid cylinder
Process	Piece by piece operation	Continuous
Temperature	Mould undergoes a temperature cycle of heating and cooling	Mould do not undergo temperature cycle
Load	Cyclical force over an area	Constant force operation, line loading
Demoulding	Mould and workpiece separation is in the direction perpendicular to the surface of the mould	Mould and workpiece separation similar to the peeling mode

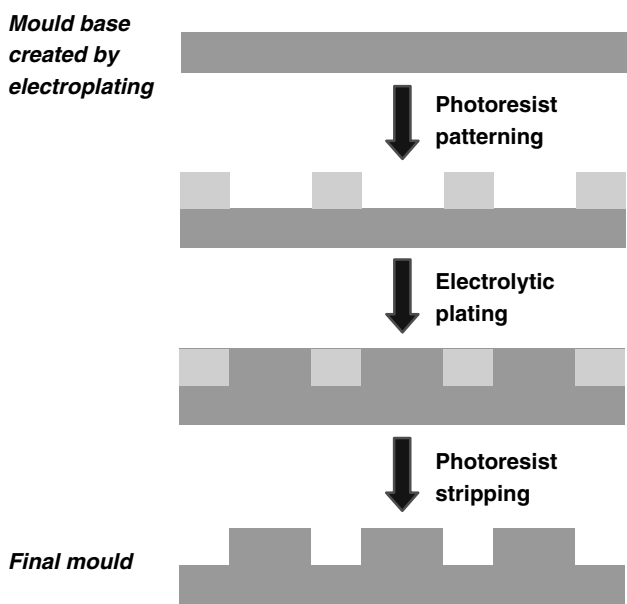


Fig. 2 Mould fabrication process

surface roughness would have to be reduced further by optimizing the parameters or changing the scheme of the electroplating. Figure 4b shows a typical profile of mould feature. A thermocouple connected to a temperature controller was embedded into the roller. The machine had a web width of 450 mm and was capable of achieving a rolling speed of up to 100 mm/s. Pneumatic pressure up to 6 bar (applied at two pneumatic pistons) provided the nip force between the rollers. Cast PMMA (Dama Enterprise)

sheets with 1.5 mm thickness were used in the experiments. The sheets were diced into sample size of 100 mm × 30 mm. Figure 5 shows some of the samples after embossing. The range of parameters used were: roller temperature (80–160°C), pneumatic pressure (1–6 bar), and linear speed (1.5–35 mm/s). The PMMA had a glass transition temperature of ~105°C measured from dynamic mechanical analysis. Some specifications of the material are given in Table 2. Stylus profilometry was used to obtain the profile and embossing depths of the PMMA features.

To test the feasibility of the hot roller embossing process on making actual microfluidic devices, an array of capillary electrophoresis separators was roller embossed on PMMA. Four 1 mm diameter holes were drilled for each separator using a machine vision assisted CNC router. The microchannels were sealed by bonding to another layer of 250 µm thick PMMA film (Goodfellow Cambridge Ltd) via a 25 µm thick, optically clear adhesive transfer film (3 M 8161). Figure 6 shows the schematic of the cross-section of the embedded microchannels. The array of devices was tested for flow by filling them with a fluorescence dye.

4 Results and discussion

The primary parameters of the process include roller temperature, loading pressure and rolling speed. As seen in Figs. 7 and 8, the embossed depths increased when pressure is increased or when the roller speed is reduced.

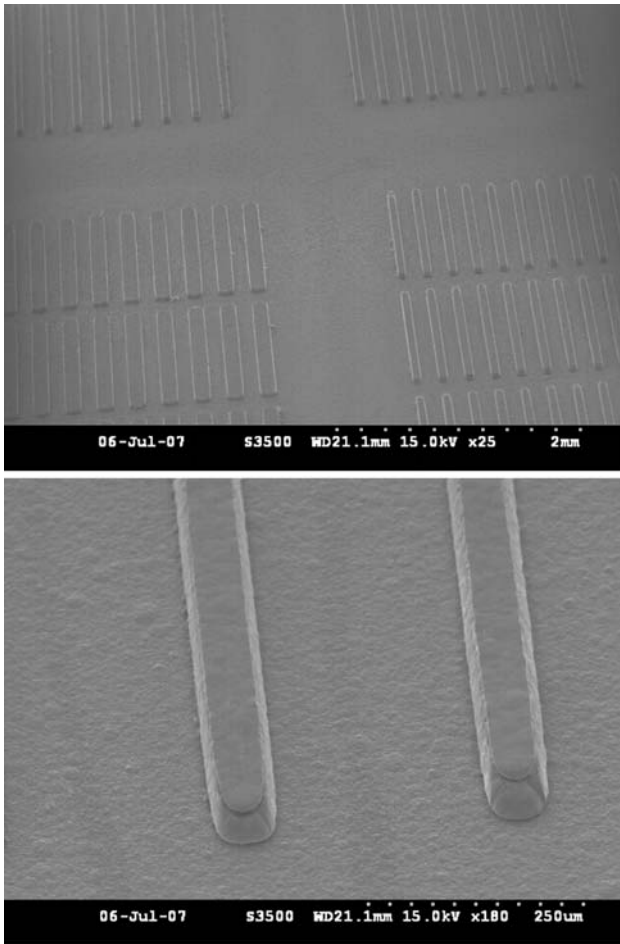


Fig. 3 Scanning electron micrographs of mould features

Fig. 4 Nickel electroplated mould features: **a** surface roughness of mould base, **b** two-dimensional profile of a feature

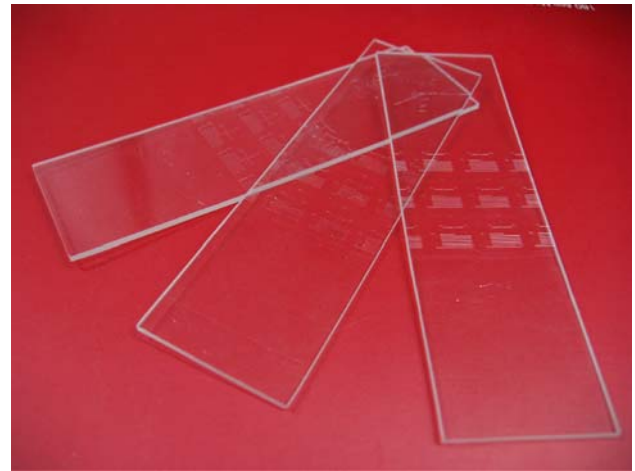
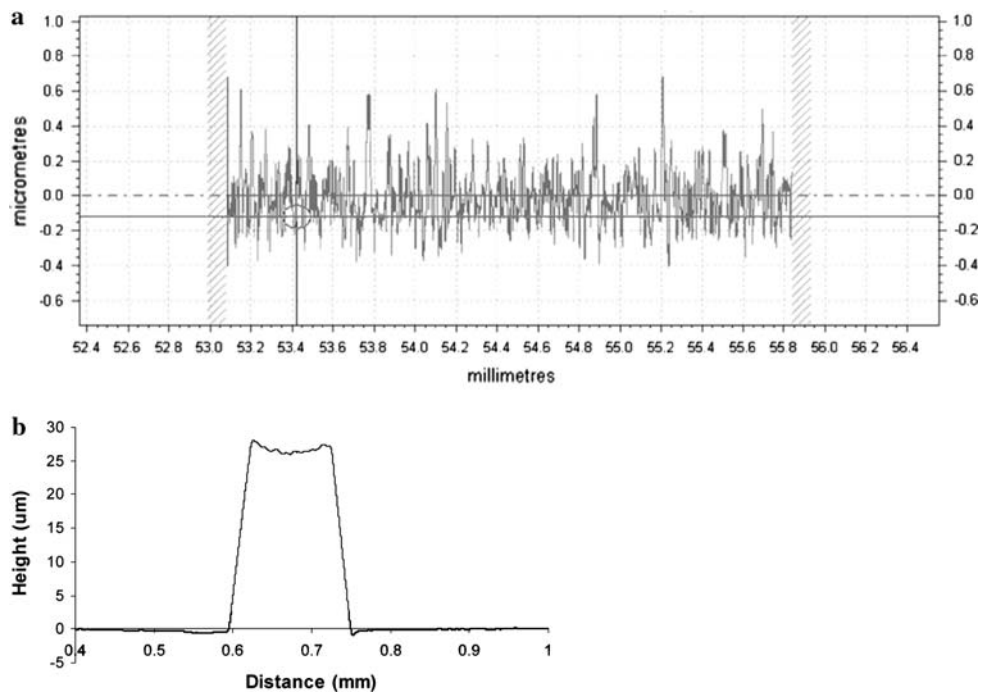


Fig. 5 Embossed PMMA samples

Table 2 Specifications of the PMMA used for roller embossing

Glass transition temperature	105°C
Specific gravity	1.19
Hardness	M-100
Tensile modulus	28,000 kg/cm ²
Coefficient of thermal expansion (linear)	$6 \times 10^{-5} \text{ K}^{-1}$

Figure 7b shows the actual nip force exerted between the rollers calibrated against the pneumatic pressure at the two pistons. In the graphs, the data points represent averages over six readings and the error bars are one standard deviation from the mean. The data were collected from a

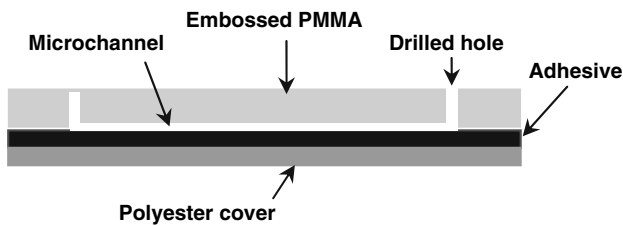


Fig. 6 Schematic showing the cross-section of a device sealed for flow testing

100 μm line array using a stylus profilometer. The mould contained positive relief features occupying a small percentage of the mould base area. Hence, initial contact between the mould and the polymer happened at the top surface of the mould features. The mechanism is then similar to indentation where a higher contact pressure will result in a larger depth of penetration. The roller speed dictates the amount of time for transient heating of the surface of the polymer that contacts the mould. A slower speed will also allow a longer time for viscoplastic flow of the polymer material. As seen in Fig. 8b, there is an

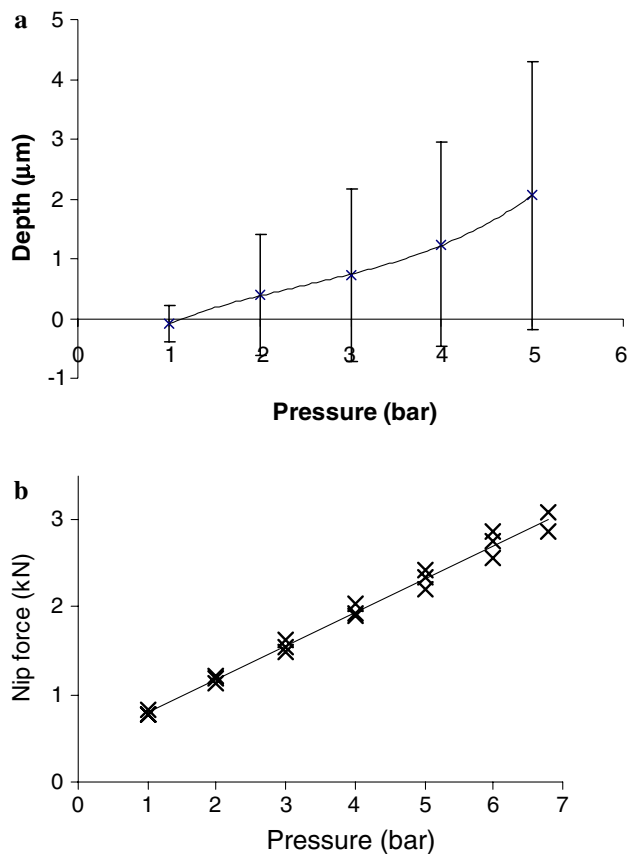


Fig. 7 Effect of load: **a** embossing depth versus pneumatic pressure applied in the pistons, **b** calibration curve of nip force versus pneumatic pressure

optimal roller temperature (around 140°C) in regards to the embossed depth. Below 110°C, the embossed depth is less than 1 μm . Although the glass transition temperature of the PMMA is 105°C, it is above 120°C that the depth starts to increase rapidly, peaking at $\sim 140^\circ\text{C}$. This is related to the pressure applied and roller speed that determines the heating time of the polymer. An interesting phenomenon is seen above 140°C where the depth starts to decrease. This could be a result of the partial reflow of the polymer material that has been heated up to a more fluidic state, after the mould separates from it. The phenomenon is not seen in rigid mould hot embossing where the demoulding is carried out at temperatures below the glass transition of the polymer, greatly reducing polymer movement after mould separation.

Figure 9a shows the profilometry scans of a 100 μm feature embossed at different temperatures from 80 to 160°C. The microchannel is running perpendicularly to the rolling direction. The depth of embossing increases with temperature. Larger increases in embossing depths were observed at temperature more than 110°C. At the same time, pile up of material at the leading and trailing edges of the feature was observed (see Fig. 9b). There is a directional effect where the pile up is much higher at the trailing edge than at the leading edge. The trailing edge pile up

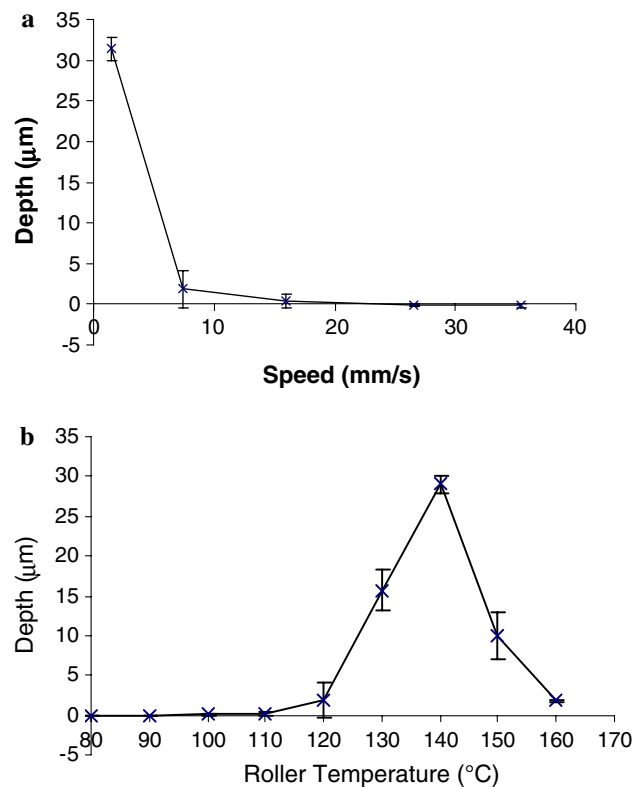


Fig. 8 Effects of **a** rolling speed and **b** roller temperature on embossed depth

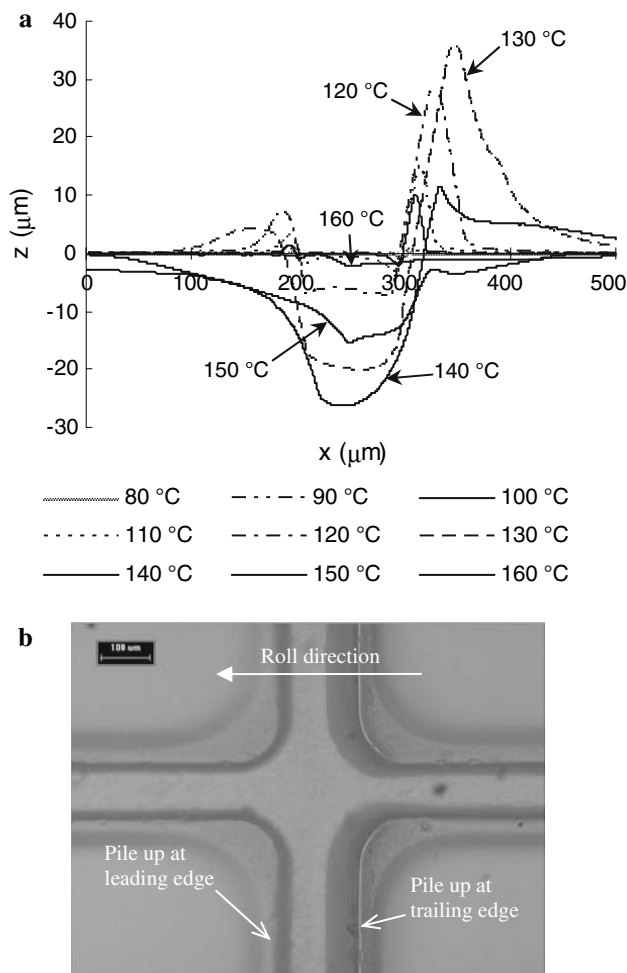


Fig. 9 Material pile up outside embossed regions: **a** two-dimensional profiles of 100 μm features embossed at different temperatures showing the asymmetrical pile up of material, **b** image showing feature embossed at 130°C

could be as much as 6 times higher than at the leading edge. Both pile up heights at the leading and trailing edges increase with temperature. At 130°C, the leading edge pile up was $\sim 4 \mu\text{m}$ while it was $\sim 35 \mu\text{m}$ at the trailing edge. Beyond 130°C, there is a decrease in both pile up heights due to the reflow effect.

A further test was conducted by rolling the mould in a reverse direction and then observing the same mould embossed feature. Figure 10a shows a typical result when comparing embossed features rolled from different directions. Both profiles were taken from two samples embossed by the same mould feature. The microchannel was running perpendicularly to the rolling direction. In the forward rolling direction, the leading edge is on the left of the graph; in the reverse rolling direction, the leading edge is on the right of the graph. The two profiles were almost a reversed image of each other as a result of the difference in rolling direction. In both cases, the material pile up was

higher on the trailing edge side than on the leading edge side of the microchannel. The difference between the two leading edge pile ups was $\sim 2.7 \mu\text{m}$ while the difference between the two trailing edge pile ups was $\sim 2 \mu\text{m}$. The difference between the two embossed depths was $\sim 2 \mu\text{m}$ taken at the midpoint of the microchannel.

While other factors such as pattern density effects could also cause asymmetric pile ups, we believe the dominant factor causing the phenomenon seen here could be due to the shear forces acting at the mould and polymer interface as a result of the configuration of the roller embossing setup. The observation was an unusually difference in pile up heights (up to a factor of ~ 6) seen when the microchannel was oriented perpendicularly to the rolling direction and which the relative (high and low) pile up positions changed with the rolling direction.

In this roller setup configuration, the rubber support roller was driven by the motor. The embossing roller was in turn driven by the support roller when the two rollers came into contact. When the polymer sheet was fed between the two rollers, the embossing roller was driven by the polymer sheet. Hence, a shear force was acting on the embossing roller by the polymer sheet in the direction of the rolling motion. At the micro level, mould features that had indented into the polymer material experienced a horizontal force in the direction of the roller motion. The compressive stresses at the trailing face of the feature could have resulted in the larger built up of material, as compared to the pile up at the leading edge. With the increase in temperature, more pile up of polymer at this trailing edge occurred as a result of the decreased resistance to flow of the polymer material. However, at higher temperatures beyond 130°C as discussed earlier, the reflow effect became dominant and caused the decrease in pile up. Pile up of material occurred when there is incomplete embossing resulting in the non contact of mould base and the polymer substrate. In cases where the mould does not contact the polymer, the field regions (outside the patterned area) of the embossed PMMA were observed to remain optically clear and smooth. Contact of the mould base with the polymer would result in the roughness of the mould embossed into the PMMA—resulting in field regions that appeared hazy. In initial studies on another machine with synchronized top and bottom rollers, we had observed this highly skewed, directional asymmetric pile up phenomenon to disappear.

For microchannels running along the rolling direction, the material pile ups on both sides were similar as seen in Fig. 10b. The difference in pile up heights on the left and right side of the microchannel was $\sim 2 \mu\text{m}$ for both forward and reverse rolling directions. This slight difference in pile up heights on both sides of the microchannel could be due to other factors rather than the effect of the rolling

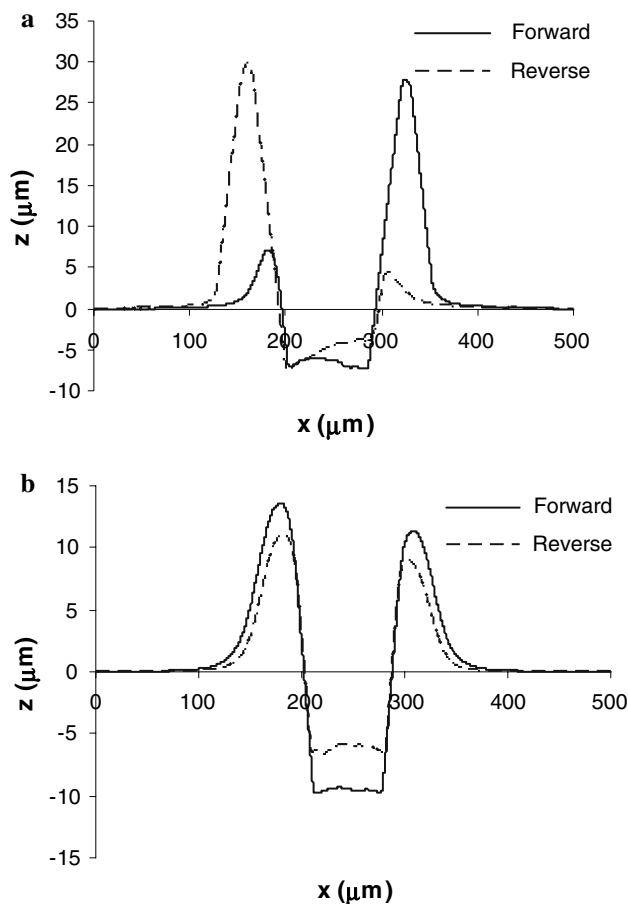


Fig. 10 **a** Effect rolling direction on material pile up as seen on the same feature. In the forward rolling direction, the leading edge is on the left of the graph; in the reverse rolling direction, the leading edge is on the right of the graph. **b** Two-dimensional profile of a microchannel traveling in the direction of the rolling showing symmetrical material pile up on both sides of the microchannel

direction because the left pile up (in the figure) was higher than that of the right for both rolling directions. The symmetrical pile up could also be observed in the image of Fig. 9b, at the horizontal section of the “cross.” Although the configuration of the embossing setup remained the same, the stresses experienced by the material on either side of the microchannel are similar as a result of the alignment of microchannel in the rolling direction.

Measurements conducted on 100 μm features showed that the lateral dimensions can be replicated to within 2% tolerance, while over 85% of mould depth is embossed. Figure 11 shows 100 μm width raised lines on the mould in comparison to the corresponding embossed PMMA microchannels. Feature sizes down to 50 μm and feature depths up to 30 μm have also been demonstrated. Figure 12a shows a three-dimensional surface profile of an embossed design of a microchannel for capillary electrophoresis. The microchannel width is 100 μm and the

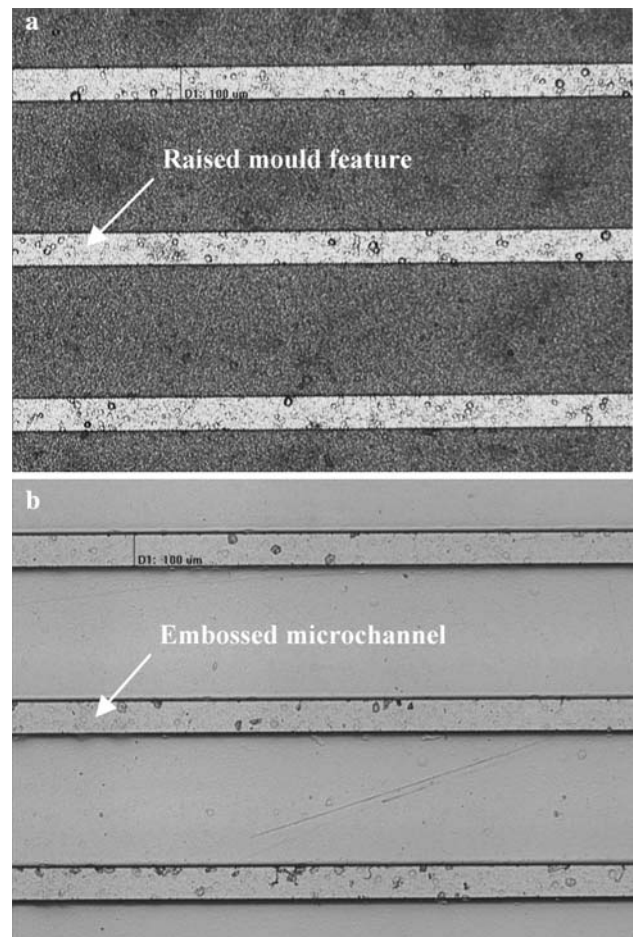


Fig. 11 **a** Mould features and **b** embossed microchannels

average depth of embossing is ~20 μm. Some pile up can still be seen especially at the edges of the microchannel, as well as warpage of the chip itself. An array of the design was also adhesively bonded to another polymer to create embedded microchannels. Holes were drilled for fluid flow in and out of each feature. Figure 12b shows the array filled with a fluorescence dye in a simple flow test.

5 Conclusions

The results demonstrated hot roller embossing of PMMA sheets with embossed feature depths that were >1 μm deep. This was possible with a compromise in the throughput. Embossed depths of more than 30 μm with 100 μm features were achieved at a speed of 1.5 mm/s. The embossed depths were within range of typical microchannel dimensions in microfluidic devices. The process could have the potential for mass production of polymer based microfluidic devices. In this research, feature sizes down to 50 μm and embossed depths of up to 30 μm had been demonstrated. An array of capillary electrophoresis separators were also created from

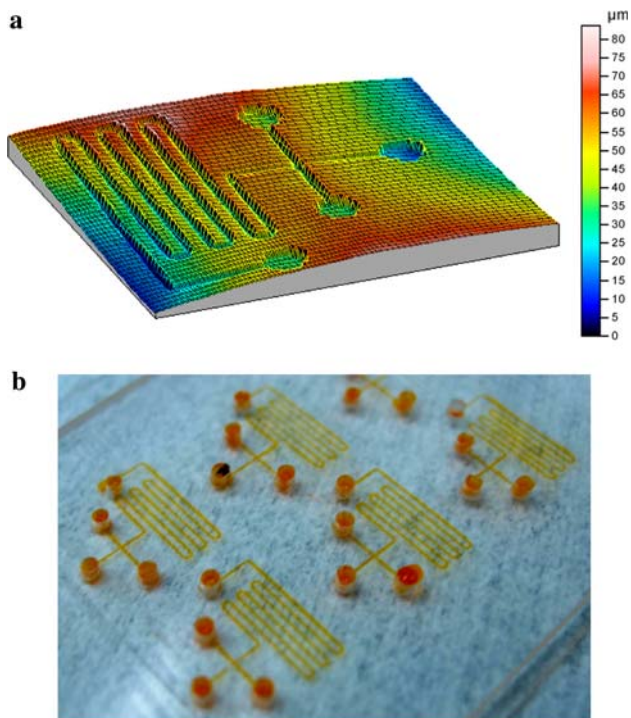


Fig. 12 Capillary electrophoresis separator fabricated by hot roller embossing: **a** three-dimensional surface profile of roller embossed structure, **b** bonded, embedded microchannels filled with fluorescence dye

the embossed structures. Flow tests were successfully conducted on this feature array.

Acknowledgments This research is funded by the Agency for Science, Technology and Research (A*STAR), Singapore.

References

- Gale MT, Gimkiewicz C, Obi S, Schnieper M, Sochtig J, Thiele H, Westenhofer S (2005) Replication technology for optical microsystems. *Opt Lasers Eng* 43:373–386. doi:[10.1016/j.optlaseng.2004.02.007](https://doi.org/10.1016/j.optlaseng.2004.02.007)
- Herzig HP (1997) *Micro-optics: elements, systems and applications*. Taylor & Francis, London
- Ng SH, Wang ZF, Tjeung RT, de Rooij NF (2007) Development of a multi-layer microelectrofluidic platform. *J Microsyst Microsyst* 13:1509–1515. doi:[10.1007/s00542-006-0341-6](https://doi.org/10.1007/s00542-006-0341-6)
- Schift H, Halbeisen M, Schutz U, Delauche B, Vogelsang K, Gobrecht J (2006) Surface structuring of textile fibers using roll embossing. *Microelectron Eng* 83:855–858. doi:[10.1016/j.mee.2006.01.120](https://doi.org/10.1016/j.mee.2006.01.120)
- Tan H, Gilbertson A, Chou SY (1998) Roller nanoimprint lithography. *J Vac Sci Technol B* 16:3926–3928. doi:[10.1116/1.590438](https://doi.org/10.1116/1.590438)